

# Additive induced polymorphous behavior of a conformationally locked hexol†

Goverdhan Mehta,\* Saikat Sen and Kailasam Venkatesan

Received 25th September 2006, Accepted 5th December 2006

First published as an Advance Article on the web 12th December 2006

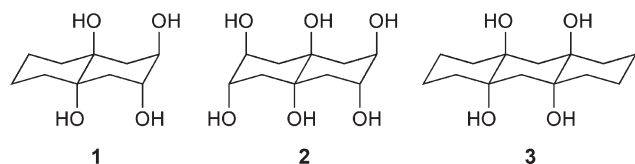
DOI: 10.1039/b613949c

The influence of molecular additives on the crystal structure adopted by a  $C_{2h}$  symmetric, conformationally locked hexol **2** forms the object of the present study. It has been observed that the polycyclitol **2** crystallizes in two polymorphic ( $\alpha$  and  $\beta$  forms) and one pseudopolymorphic (monohydrate) modification, depending on the presence and nature of the additive employed. Thus, with the sole exception of trimesic acid, which induces **2** to crystallize in the denser  $\beta$  form, the molecular additives screened in this study either failed to promote polymorphism in **2** or caused it to crystallize as a monohydrate. The putative role of trimesic acid in providing an alternate crystallization pathway to the polyol **2** has been discussed.

## Introduction

For quite some time now, we have been involved in the synthesis and crystal structure elucidation of conformationally locked polycyclitols with the objective of developing an insight into their unique supramolecular architecture.<sup>1</sup> As compared to their monocyclic siblings, such as monosaccharides and inositols, conformationally locked polycyclitols (a portmanteau word derived from ‘polycyclic cyclitol’)<sup>2</sup> are destined to exhibit a ground-state *axial rich* disposition of the hydroxyl groups on account of their rigid *trans*-decalin backbone. This peculiar aspect of their molecular structure permits one to conceive of the spatial dispositions of the O–H $\cdots$ O H-bond<sup>3</sup> donors and acceptors in the locked polyol as virtually unaffected by crystal effects.

This concept was put into effect while studying the crystal packing in three specially crafted conformationally locked polyols **1–3** (Scheme 1), in which intramolecular H-bonding between the 1,3-diaxial OH groups causes the molecules to behave much like LEGO<sup>®</sup> bricks in the supramolecular world with preordained positions of intermolecular O–H $\cdots$ O H-bond donors and acceptors.<sup>4</sup> This facet of their molecular structure not only simplified a qualitative visualization of the various packing patterns in **1–3**, but also allowed us to propose, based on previously reported CSD analyses, the packing motifs most likely to converge with the experimental results. Among the



Scheme 1

Department of Organic Chemistry, Indian Institute of Science, Bangalore, 56012, India. E-mail: gm@orgchem.iisc.ernet.in; Fax: +91-80-23600283; Tel: +91-80-22932850

† Electronic supplementary information (ESI) available: DSC characteristics and SPE comparison for the two forms of **2**, along with details of molecular packing in the  $\alpha$  form. See DOI: 10.1039/b613949c

three polyols **1–3** studied above, the bicyclic  $C_{2h}$  symmetric hexol **2**, with its *all axial* disposition of the six hydroxyl functionalities, presented itself as a structurally novel polycyclitol molecule. Although the O–H $\cdots$ O hydrogen bonded packing motif, determined experimentally for **2**, was in conformity with proposed packing patterns, it appeared worthwhile to investigate the alternate modes of molecular association that may be accessed by **2** under suitable crystallization conditions. Implicit in this expectation was a desire to gain an insight into the extent of flexibility that may be exhibited by a conformationally locked polyol, like **2**, in the choice of packing motif. The present article is intended to disclose our observations in this pursuit.

## Results and discussion

Following the synthetic sequence, previously reported,<sup>4</sup> the polycyclitol **2** was obtained as a white microcrystalline powder, starting from a readily available aromatic precursor naphthalene. Powder X-ray diffraction pattern recorded on a finely ground bulk sample of the polyol **2** matched with that simulated for the crystal structure of **2** that has been recently reported (the  $\alpha$  form) (Fig. 1).<sup>4</sup> Our initial attempts towards inducing polymorphism in **2** involved routine crystallization checks under ambient conditions in solvents of varying nature and polarity, such as methanol, ethanol, ethyl acetate, acetone and acetonitrile.<sup>5</sup> However, in all of these crystallization attempts, the polyol **2** either failed to produce single crystals or packed in the  $\alpha$  form.<sup>4</sup> At this stage it was felt that introduction of molecular additives, capable of interacting with the polycyclitol **2** through O–H $\cdots$ O interactions during the crystallization process, might alter the mode of self-recognition in **2** and thus generate a different supramolecular assembly.<sup>5,6</sup> Competing formation of a supramolecular complex between the polyol and the additive was a viable possibility which was not entirely ruled out at this point.

In this regard, the commonly available and well known co-crystallization agent and molecular additive, trimesic acid **4**, was chosen for the initial foray.<sup>7,9</sup> All the crystallization

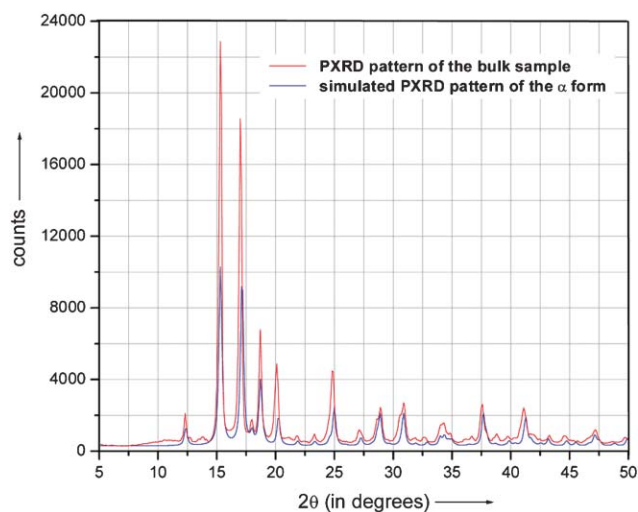


**Fig. 1** Comparison of the powder X-ray diffraction pattern recorded for a bulk sample of **2** with that simulated for the  $\alpha$  form.

attempts were performed in 10 mL Pyrex<sup>®</sup> Erlenmeyer flasks with 8–10 mg ( $\approx 0.03$ – $0.04$  mmol) of the hexol **2**, employing the same batch of distilled solvents and under as nearly identical ambient conditions as possible. Crystals of **2** were grown from their *dilute* solutions in 1 : 1 : 2 methanol–ethanol–ethyl acetate solvent system in the presence of dissolved trimesic acid, present in mole ratios (acid : polyol) 1 : 10, 1 : 5, 1 : 2.5 and 1 : 1. Typically, 5 to 7 crystals of the hexol **2** were obtained from the milieu in each case. In a definitive contrast to the crystals of **4**, which were rather small and ill-defined in their morphology, those of the polyol **2** were large with well-defined faces and could thus be clearly made out under an optical microscope. With lower proportions of the acid **4**, the hexol **2** crystallized solely in the  $\alpha$  form with its characteristic cuboidal block-like morphology. In the presence of a 1 : 1 mole ratio of **4** : **2**, however, the polyol **2** was found to adopt a different external habit (the  $\beta$  form) which could be perceived, under close observation, as being still cuboidal but somewhat plate-like when compared to the crystals of the  $\alpha$  form (Fig. 2).

Single crystal X-ray diffraction analysis performed on *all* the crystals of **2** obtained under these conditions, confirmed that the  $\beta$  form represented, in fact, a different polymorphic modification of the polyol **2**.<sup>5</sup> While packing in the same centrosymmetric monoclinic space group ( $P2_1/n$ ,  $Z = 2$ ) as the  $\alpha$  form, the  $\beta$  form represented not only a more dense crystalline phase of the hexol **2**, but also a more stable one as judged from the DSC studies and single point energy calculations on the packing motifs of the two polymorphs of **2**.<sup>8</sup> On the whole, the packing pattern in the  $\beta$  form of **2** bore salient points of resemblance to that observed in the  $\alpha$  form. In either polymorph, each intramolecularly H-bonded  $C_{2h}$  symmetric molecule of the hexol **2** occupies a crystallographic inversion center and links to its nearest neighbors with four intermolecular O–H $\cdots$ O bonds to form hydrogen bonded tapes, exhibiting a characteristic centrosymmetric tetrameric arrangement of hexol molecules (Fig. 3, Table 1).<sup>4,8</sup>

However, a closer examination of the packing motifs in the two modifications of **2** made evident the subtle differences that

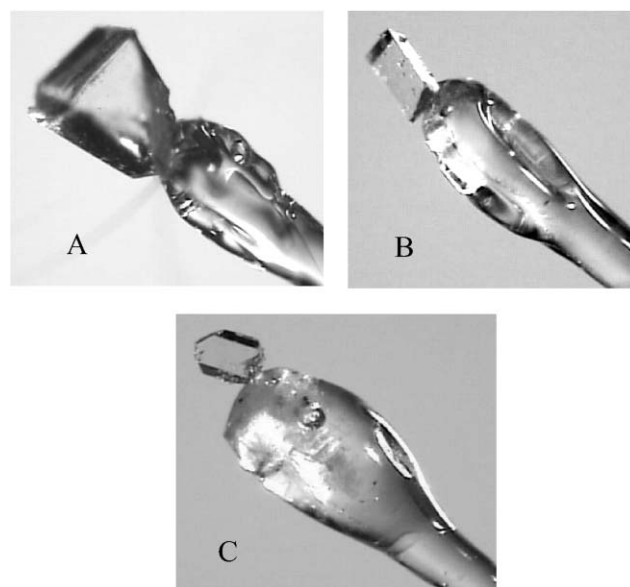


**Fig. 2** Photographs of the representative crystals of (A) the  $\alpha$  form, (B) the  $\beta$  form and (C) the monohydrate of **2**.

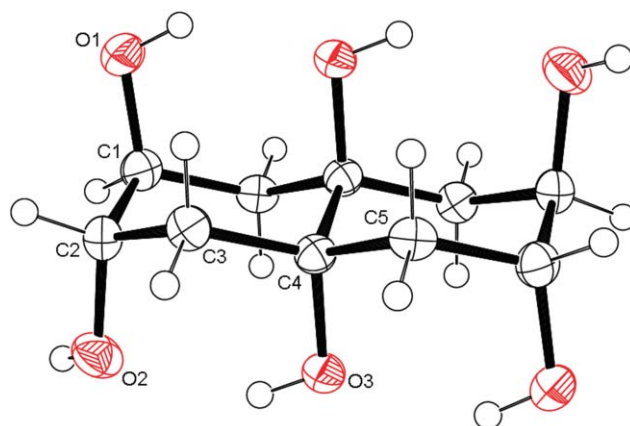


**Fig. 3** ORTEP diagram of the  $\beta$  form of **2**, with the atom numbering scheme for the asymmetric unit. Displacement ellipsoids have been drawn at 50% probability level and H atoms are shown as small spheres of arbitrary radii. The unlabelled atoms are related to the labelled atoms by the symmetry code ( $1 - x, 2 - y, 2 - z$ ).

**Table 1** Hydrogen bond geometry in the  $\beta$  form of **2**

D–H $\cdots$ A	D–H/Å	H $\cdots$ A/Å	D $\cdots$ A/Å	D–H $\cdots$ A/ $^\circ$
O1–H10 $\cdots$ O3 <sup>i</sup>	0.82	1.97	2.6695(15)	142
O2–H20 $\cdots$ O1 <sup>ii</sup>	0.82	1.97	2.8074(16)	164
O3–H30 $\cdots$ O2 <sup>iii</sup>	0.82	1.97	2.7228(15)	147

<sup>a</sup> Symmetry codes: (i)  $1 - x, 2 - y, 2 - z$ ; (ii)  $1/2 - x, 1/2 + y, 3/2 - z$ ; (iii)  $x, y, z$ .

exists between them. Thus, while intermolecular H-bonds in the  $\alpha$  form connect molecules of **2** related by  $2_1$  symmetry to form tapes growing normal to the (1 0 1) direction, those in the  $\beta$  form link the ones related by the  $n$  glide to generate molecular tapes perpendicular to the (2 0  $-2$ ) direction (Fig. 4).<sup>4,8</sup>

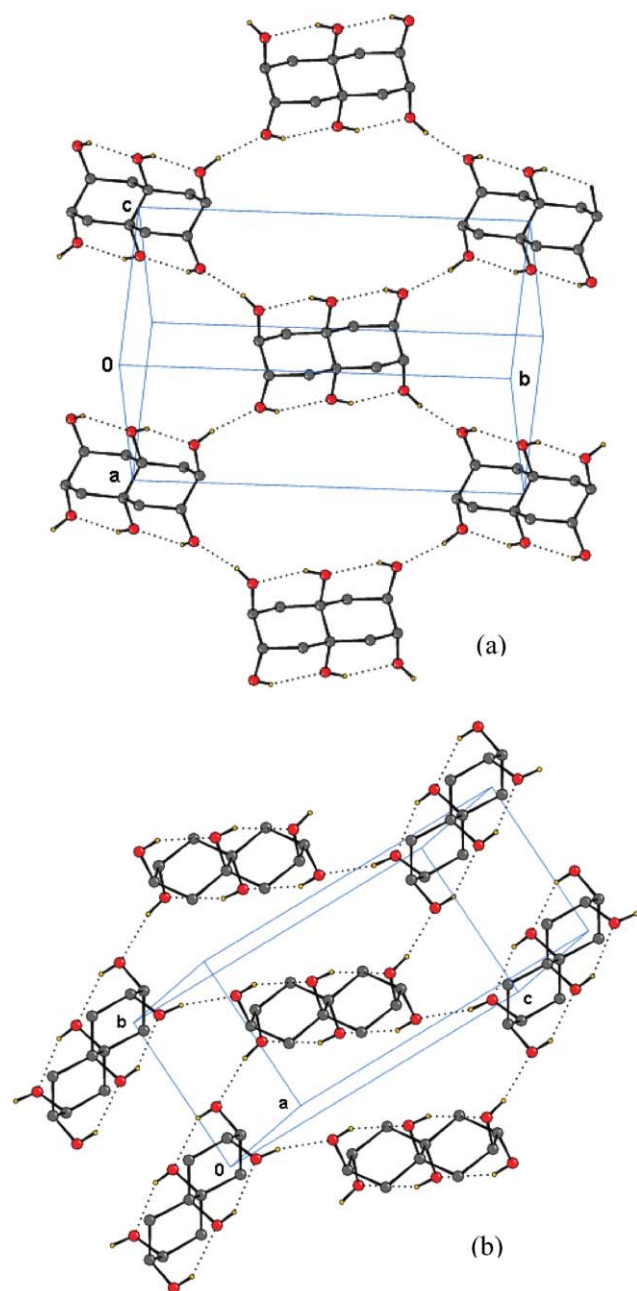


**Fig. 4** Molecular packing in (a) the  $\alpha$  form, and (b) the  $\beta$  form of the hexol **2**. Hydrogen atoms bonded to carbon atoms have been omitted for clarity.

In addition, the packing motifs of the two polymorphs of **2** also exhibited significant differences in their intermolecular O–H $\cdots$ O bond angles ( $\alpha$  form, 169°;  $\beta$  form, 164°) and C–O–H $\cdots$ O dihedrals ( $\alpha$  form, 36°;  $\beta$  form, 103°) (Fig. 5). Indeed these differences in the self-assembling process of **2**, though seemingly minor, get reflected significantly in a closer packing of molecules in the  $\beta$  form as compared to the  $\alpha$  form. The situation can be likened to an apparent ‘squeezing’ of the crystalline lattice in going from the  $\alpha$  to the  $\beta$  form of **2**.

Intrigued by the formation of a polymorphic modification of **2** under very specific crystallization protocols (1 : 1 molar ratio of **4** : **2**), we felt encouraged to explore the possibility

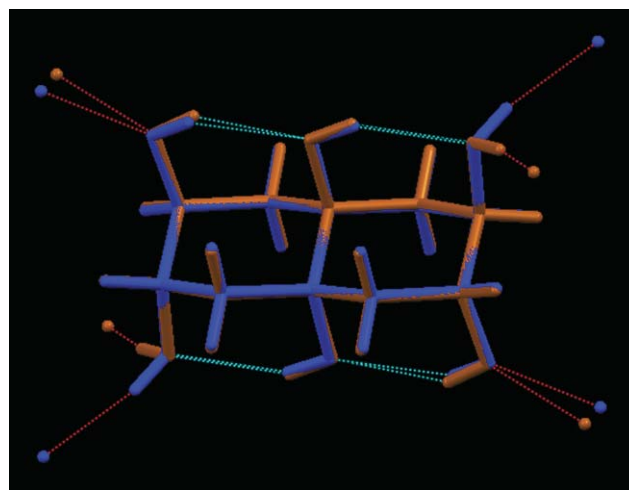


**Fig. 5** Overlay of molecules of the hexol **2** in the  $\alpha$  (blue) and the  $\beta$  (orange) forms. Note the prominent change in the C–O–H $\cdots$ O dihedral angles in the two polymorphs.

of employing other additives, possessing either the carboxyl functionality or a three-fold symmetric disposition of H-bond donors (and/or acceptors) as **4**, to generate either the  $\beta$  form or some other polymorph of **2**. Accordingly, the crystallization experiments described above were repeated using benzoic acid, phthalic acid, isophthalic acid, terephthalic acid, boric acid, phloroglucinol dihydrate (crystallization was carried out in an amber colored flask in this case, owing to light sensitivity of the additive) and cyanuric acid as molecular additives.<sup>9</sup> As observed in case of trimesic acid, all the additives crystallized under these conditions either as clustered microcrystals or in the form of ill-defined scales and fibres, thereby easing considerably the task of separation of the crystals of **2** from the above. With all three isomeric benzene dicarboxylic acids and phloroglucinol, the hexol **2** crystallized solely in the  $\alpha$  form. Interestingly, when present in equimolar ratio with each of the remaining three additives, the polycyclitol **2** was found to crystallize with a hexagonal prismoid morphology (Fig. 2). X-Ray diffraction data collected on *all* the crystals of **2** obtained under these conditions (typically 9–10 per batch), revealed that the latter represented a monohydrate (a pseudopolymorph) of the hexol **2** in the centrosymmetric triclinic space group ( $P\bar{1}$ ,  $Z = 2$ ).<sup>5b,10</sup> Analysis of the crystal structure of the monohydrate revealed that the asymmetric unit contains two molecules of **2** (A and B), occupying the inversion centers at  $(0, \frac{1}{2}, 0)$  and  $(\frac{1}{2}, \frac{1}{2}, \frac{1}{2})$ , and a water molecule, lying in a general position (Fig. 6).

Each of the intramolecularly H-bonded hexol molecules of one type is linked through four intermolecular O–H $\cdots$ O hydrogen bonds to two hexol molecules of the other type and two water molecules to form hydrogen bonded tapes growing perpendicular to the  $(4\ 2\ 0)$  direction. The H-bonded supramolecular tapes thus generated are connected through intermolecular O–H $\cdots$ O hydrogen bonds, involving the water molecules of one tape and the B-type molecules of the succeeding and preceding ones (Table 2, Fig. 7 and 8).

The assembly of molecules in each tape of the hydrate bears an unmistakable resemblance to the one that might

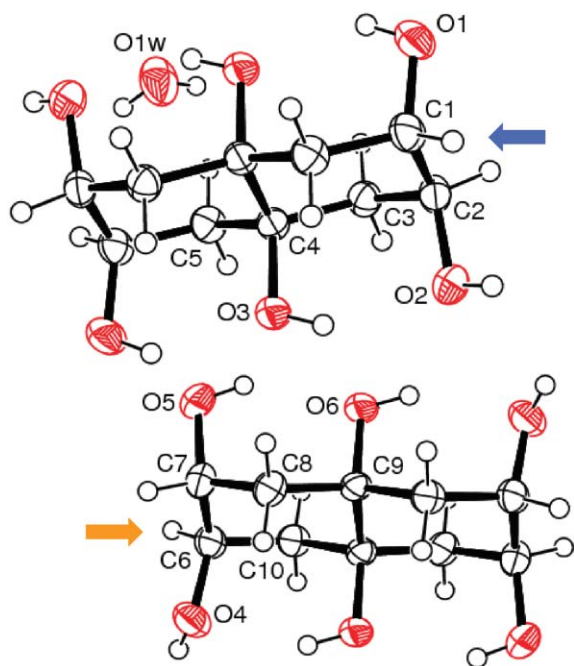


**Fig. 6** ORTEP diagram of the monohydrate of **2**, with the atom numbering scheme for the asymmetric unit. Displacement ellipsoids have been drawn at 50% probability level and H atoms are shown as small spheres of arbitrary radii. The A and B type of hexol molecules have been indicated by orange and blue arrows respectively. The unlabelled atoms are related to the labelled atoms by the symmetry codes  $(2 - x, 1 - y, 2 - z)$  and  $(1 - x, 1 - y, 1 - z)$  for molecules of A and B types respectively.

be generated intuitively from the tetrameric arrangement of hexol molecules, present in either polymorph of **2**, after the incorporation of two molecules of water across its center of symmetry (see Fig. 9 for overlay diagrams of individual molecules of the hexol **2** and their packing in the monohydrate and the  $\alpha$  form). As a consequence, there is an increased void space within the crystalline lattice of the hydrate, resulting in a lowering of density as compared to either modifications of **2**. Indeed, comparison of the packing patterns of the two polymorphs and the pseudo-polymorph (hydrate) of the hexol **2** tempts one to draw an analogy to a cork (the  $\alpha$  form), which is capable of being squeezed (the  $\beta$  form) or swelling upon imbibing water (the hydrate).

**Table 2** Hydrogen bond geometry in the monohydrate of **2**

D-H...A	D-H/ $\text{\AA}$	H...A/ $\text{\AA}$	D...A/ $\text{\AA}$	D-H...A/ $^\circ$
O1-H1O...O3 <sup>i</sup>	0.82	2.01	2.7086(17)	142
O2-H2O...O5 <sup>ii</sup>	0.82	1.88	2.7010(18)	174
O3-H3O...O2 <sup>iii</sup>	0.82	2.00	2.7205(17)	147
O4-H4O...O1W <sup>iv</sup>	0.82	1.89	2.688(2)	164
O5-H5O...O6 <sup>v</sup>	0.82	2.03	2.7157(17)	141
O6-H6O...O4 <sup>v</sup>	0.82	2.00	2.7282(18)	148
O1W-H1W...O2 <sup>vi</sup>	0.82(3)	2.05(3)	2.856(3)	167.15(2)
O1W-H1W...O1 <sup>vii</sup>	0.82(3)	1.97(3)	2.757(2)	165.88(2)

<sup>a</sup> Symmetry codes: (i)  $1 - x, 1 - y, 1 - z$ ; (ii)  $x, y - 1, z$ ; (iii)  $x, y, z$ ; (iv)  $x, y, z + 1$ ; (v)  $2 - x, 1 - y, 2 - z$ ; (vi)  $2 - x, 1 - y, 1 - z$ ; (vii)  $x, y + 1, z$ .

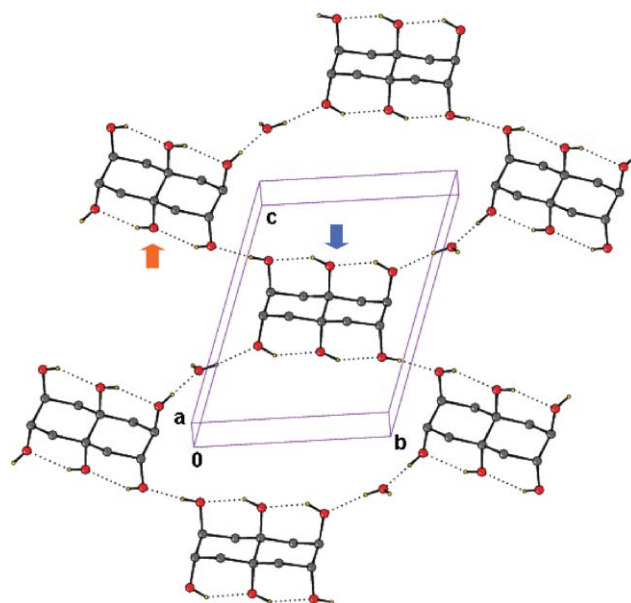


**Fig. 7** Molecular packing in the monohydrate of the hexol **2**, showing the details of a O-H...O hydrogen bonded tape. One of the A and B type molecules in the packing pattern has been indicated by orange and blue arrows respectively.

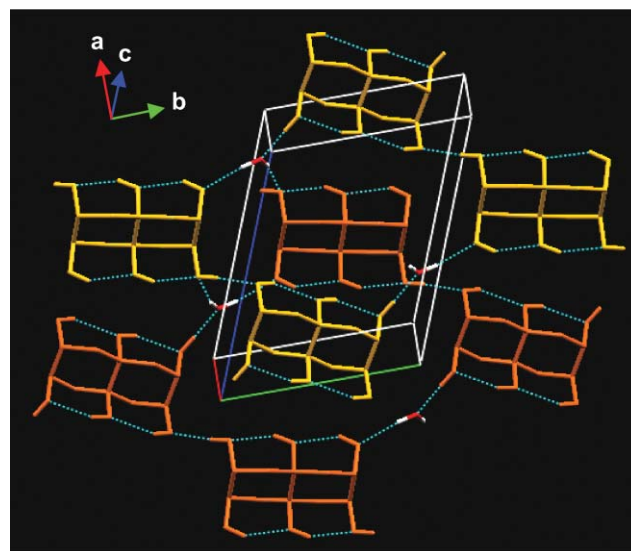


**Fig. 8** Molecular packing in the monohydrate of the hexol **2**, showing the details of the O-H...O interconnectivity between two translationally related hydrogen bonded tapes (indicated by different coloring of the constituent hexol molecules). H-atoms bonded to C-atoms have been omitted for clarity.

### What is the role of trimesic acid? A possible mechanism for crystal nucleation

The fact that the denser and more stable  $\beta$  form of the hexol **2** was obtained in the present study solely in the presence of trimesic acid, an additive structurally dissimilar to **2**, is intriguing and therefore, throws open for speculation the precise role played by the molecular additive in the self-recognition process of the polyol **2**. Even though the observed

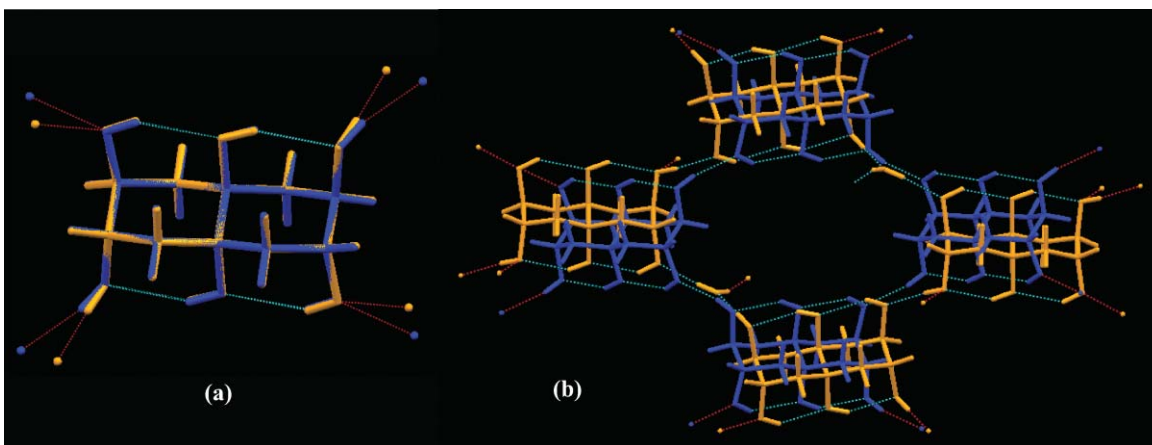


Fig. 9 Overlay of (a) individual molecules of the hexol **2** and (b) their packing in the  $\alpha$  form (blue) and the monohydrate (yellow) forms.

phenomenon could well have been the overall manifestation of a number of indeterminate factors, a putative rationale for the polymorphic behavior of **2** can still be forwarded if one were to assume that **4** forms the seeding nuclei for the hexol **2** during the formation of the  $\beta$  form. Logically, the foregoing proposition is more likely to gain credence in cases where the crystallization milieu attains an earlier saturation in **4**. Hence, given that **2** and **4** differed only slightly in their solubility in the solvent system employed for crystallization, isolation of the  $\beta$  form of **2** exclusively in the presence of an equimolar ratio of trimesic acid justifies the assumption proposed above.

As reported by Duchamp and Marsh, trimesic acid (**4**) crystallizes in the centrosymmetric monoclinic space group  $C2/c$  ( $a = 26.520(2)$  Å,  $b = 16.420(1)$  Å,  $c = 26.551(2)$  Å,  $\beta = 91.53(1)^\circ$ ,  $Z = 48$ ).<sup>9a</sup> Employing the well-known carboxylic acid dimer synthon in a characteristic pleated ‘chicken wire’ supramolecular framework, molecules of **4** form parallel O–H $\cdots$ O hydrogen bonded molecular arrays, approximately perpendicular to either the  $a$  or  $c$  axis. Consequently, the  $\{200\}$  and  $\{002\}$  faces appear as the most prominent ones in the crystal morphology of **4**, predicted by the Bravais, Friedel, Donnay and Harker (BFDH) algorithm (Fig. 10).<sup>11</sup>

Assuming that the BFDH morphology, calculated for **4**, holds good even for an embryonic crystal of the same, it is quite likely that the larger  $\{200\}$  and  $\{002\}$  crystal faces, exhibiting the highest concentration of O–H $\cdots$ O hydrogen bond donors and acceptors, in the seeding nuclei of **4** will provide the preferred attachment sites for molecules of **2**. With a congenial geometric matching and favorable O–H $\cdots$ O H-bonding between the nucleus (**4**) and the hexol (**2**) at the crystallization interface, *i.e.*  $\{200\}$  or  $\{002\}$ , a sustainable epitaxial growth of the polyol molecules on the trimesic acid template may be achieved, leading to the exclusive formation of the thermodynamically more stable  $\beta$  form (Fig. 11).<sup>12</sup> The foregoing mechanism of crystal nucleation and growth in **2**, in the presence of **4**, derives support not only from the close similarity between **2** and **4** in their space group symmetry and the characteristic interfacial angle  $\beta$ , but also from the fact that the principal supramolecular assembly through O–H $\cdots$ O H-bonding in the  $\beta$  form of **2** occurs along the  $(002)$  direction (*i.e.* along the longest axis  $c$ ) (Fig. 12).

It is quite likely that such a template-directed growth of hexol molecules might not have been sustainable in the case of the additives, other than **4**, which were employed in the present study. This might have possibly been due to an unavailability of a suitable crystal face or favorable attachment site on the nucleus, formed by the additive, for the epitaxial growth of the hexol molecules. An unfavorable and thus short-lived template-directed crystal growth, leading to the formation of a hitherto unknown polymorph of **2** possessing a lower stability than the  $\alpha$  form, could also have been a probable scenario. While these may be considered as likely explanations to the isolation of the  $\alpha$  form in the case of the three isomeric benzene dicarboxylic acids and phloroglucinol, formation of the crystalline monohydrate of the hexol **2** in presence of benzoic, boric and cyanuric acids can largely be ascribed to the hygroscopic nature of the three molecular additives and prolonged exposure to air during crystallization.

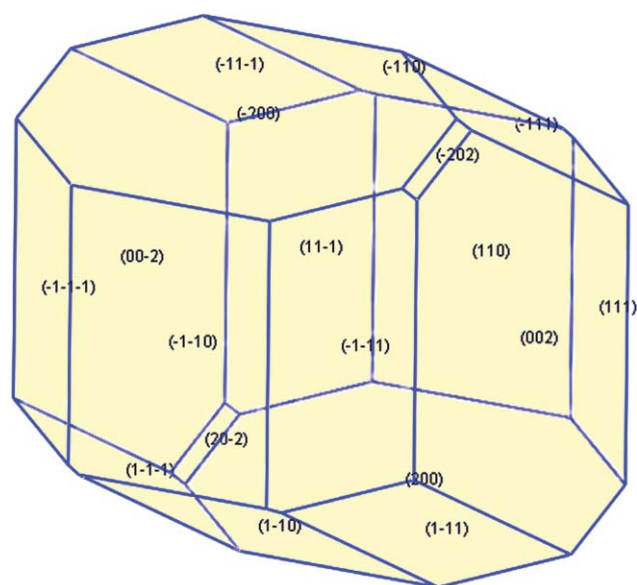
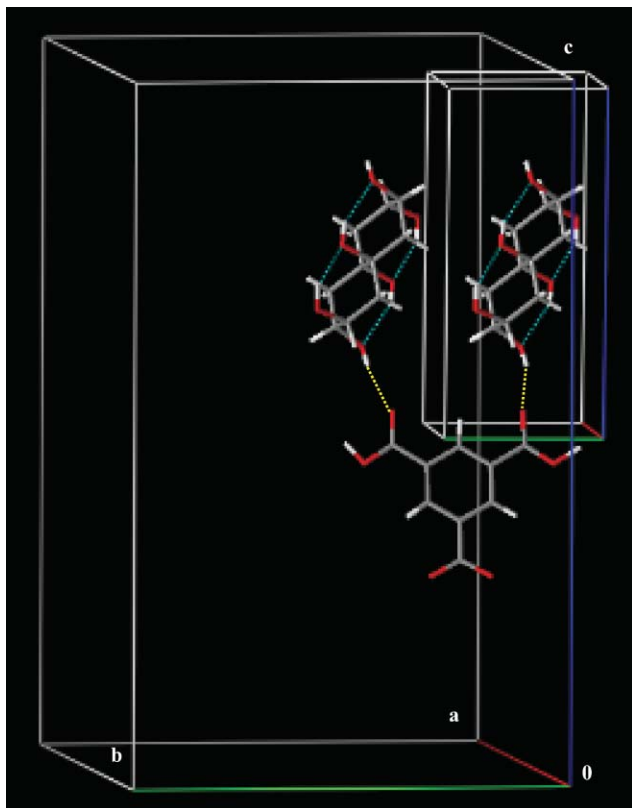


Fig. 10 BFDH morphology of trimesic acid, showing the  $(hkl)$  indices of the respective crystal faces.



**Fig. 11** A possible manner in which epitaxial growth of the hexol molecules might have taken place on the {002} crystal face of trimesic acid. The yellow dotted lines represent the O–H···O hydrogen bonds between the trimesic acid template and the molecules of **2**, while blue ones denote the intramolecular O–H···O H-bonds that exists in each hexol molecule (possibly even in solution). Note the close similarity between the interfacial angles  $\beta$  in the unit cells of trimesic acid (the larger one) and the polyol **2**.

## Experimental

### General procedures

All molecular additives employed in the present study were purchased from either Sigma-Aldrich or Fluka. Powder X-ray diffraction data was collected using  $\text{CuK}\alpha$  radiation with a scan speed of  $1^\circ \text{ min}^{-1}$  on a Siemens D5005 X-ray diffractometer, operating at 25 kV and 30 mA. The DSC data were recorded on a Mettler Toledo STAR<sup>o</sup> system. DFT single point energy calculations on the packing motifs in the two polymorphs of **2** were performed with the Gaussian 03 program package using B3LYP/6–31G\*\* basis set.<sup>14</sup>

### X-Ray crystallography

The single crystal X-ray diffraction data were collected on a Bruker AXS SMART APEX CCD diffractometer at 296 K. The X-ray generator was operated at 50 kV and 35 mA using  $\text{MoK}\alpha$  radiation. The data was collected with an  $\omega$  scan width of  $0.3^\circ$ . A total of 606 frames per set were collected using SMART<sup>15</sup> in three different settings of  $\varphi$  ( $0^\circ$ ,  $90^\circ$  and  $180^\circ$ ) and four different settings of  $\varphi$  ( $0^\circ$ ,  $90^\circ$ ,  $180^\circ$  and  $270^\circ$ ) (in case of a triclinic crystal system), keeping the sample to detector distance of 6.062 cm and the  $2\theta$  value fixed at  $-25^\circ$ . The data

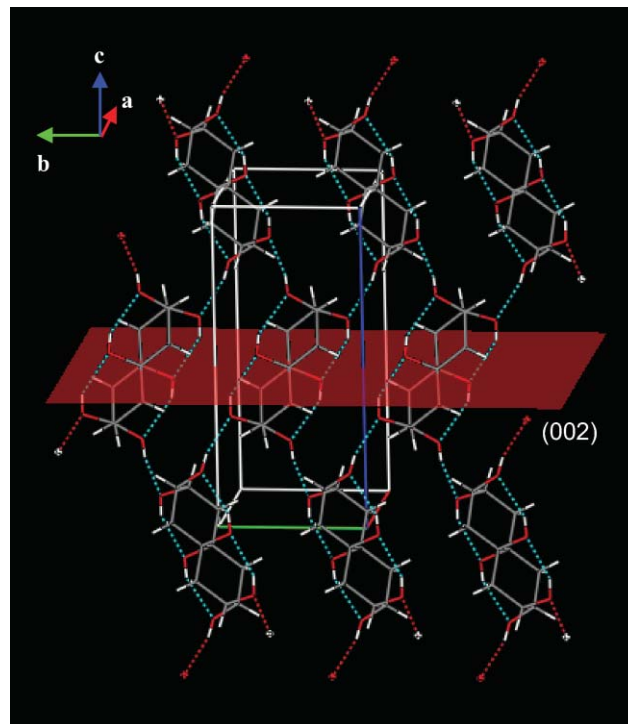


**Fig. 12** The principal supramolecular assembly through O–H···O hydrogen bonding in the  $\beta$  form of **2** occurring parallel to the (002) direction.

were reduced by SAINTPLUS;<sup>15</sup> an empirical absorption correction was applied using the package SADABS<sup>16</sup> and XPREP<sup>15</sup> was used to determine the space group. The crystal structures were solved by direct methods using SIR92<sup>17</sup> and refined by full-matrix least-squares method using SHELXL97.<sup>18</sup> Molecular and packing diagrams were generated using ORTEP32,<sup>19</sup> CAMERON<sup>20</sup> and MERCURY<sup>21</sup> respectively. The geometric calculations were done by PARST<sup>22</sup> and PLATON.<sup>23</sup> All hydrogen atoms were initially located in a difference Fourier map. The methine (CH) and methylene ( $\text{CH}_2$ ) H atoms of the hexol then were placed in geometrically idealized positions and allowed to ride on their parent atoms with C–H distances in the range 0.97–0.98 Å and  $U_{\text{iso}}(\text{H}) = 1.2U_{\text{eq}}(\text{C})$ . The O–H hydrogen atoms were constrained to an ideal geometry with O–H distances fixed at 0.82 Å and  $U_{\text{iso}}(\text{H}) = 1.5U_{\text{eq}}(\text{O})$ , but each hydroxyl group was allowed to rotate freely about its C–O bond. The positions of the H atoms of the water molecule in the monohydrate were refined freely, along with an isotropic displacement parameter.

**Crystal data for the  $\beta$  form of **2**.**  $\text{C}_{10}\text{H}_{18}\text{O}_6$ ,  $M = 234.24$ , monoclinic, space group  $P2_1/n$ ,  $a = 6.5273(14)$  Å,  $b = 5.9589(12)$  Å,  $c = 13.166(3)$  Å,  $\beta = 90.163(3)^\circ$ ,  $V = 512.10(19)$  Å<sup>3</sup>,  $Z = 2$ ,  $\rho_{\text{calcd}} = 1.519 \text{ g cm}^{-3}$ ,  $F(000) = 252$ ,  $\mu = 0.125 \text{ mm}^{-1}$ ,  $R = 0.0358$ ,  $wR = 0.0759$ , GOF = 1.089 for 953 reflections with  $I > 2\sigma(I)$ ,

**Crystal data for the monohydrate of **2**.**  $\text{C}_{10}\text{H}_{18}\text{O}_6 \cdot \text{H}_2\text{O}$ ,  $M = 252.26$ , triclinic, space group  $P\bar{1}$ ,  $a = 6.663(2)$  Å,  $b = 9.045(3)$  Å,  $c = 10.707(3)$  Å,  $\alpha = 72.385(5)^\circ$ ,  $\beta = 81.655(5)^\circ$ ,  $\gamma = 69.238(5)^\circ$ ,  $V = 574.6(3)$  Å<sup>3</sup>,  $Z = 2$ ,  $\rho_{\text{calcd}} = 1.458 \text{ g cm}^{-3}$ ,

$F(000) = 272$ ,  $\mu = 0.124 \text{ mm}^{-1}$ ,  $R = 0.0389$ ,  $wR = 0.1034$ ,  $GOF = 1.034$  for 2187 reflections with  $I > 2\sigma(I)$ ,

CCDC reference numbers 620926 and 620927. For crystallographic data in CIF or other electronic format see DOI: 10.1039/b613949c

## Conclusions

In words of the often quoted statement about polymorphism by McCrone, 'every compound has different polymorphic forms and that, in general, the number of forms known for a given compound is proportional to the time and money spent in research on that compound'.<sup>13</sup> The present study however attempts to explore through the manifestation of polymorphism, the limits of flexibility inherent in the supramolecular organization of even conformationally locked polycyclitols endowed with a rigid covalent backbone and predetermined positions of intermolecular O–H···O H-bond donors and acceptors. The results also highlight the significant role played by a seemingly structurally unrelated additive in providing an alternate nucleating pathway to facilitate the formation of an elusive polymorph during the crystallization process of a given compound. Though speculative, a putative mechanism of crystal nucleation, leading to formation of the  $\beta$  form of the hexol **2**, has been proposed in this context. Through appropriate variation in the chemical and structural parameters of the molecular additives, the experimental results detailed above may be extended to discern their intervention in the self-recognition process of other related molecules.

## Acknowledgements

We thank DST, India for the CCD facility at IISc, Bangalore, and the Supercomputer Education and Research Center (SERC) at IISc for providing the necessary computational facilities. We sincerely acknowledge the help extended by Mr Anirban Chakraborty and Ms Prangya Parimita Sahoo in recording the PXRD data for the bulk sample of **2**. GM thanks CSIR, India for research support and the award of the Bhatnagar Fellowship.

## References and notes

- (a) G. Mehta, S. Sen and S. Dey, *Acta Crystallogr., Sect. E: Struct. Rep. Online: Struct. Rep. Online*, 2005, **61**, o920; (b) G. Mehta, S. Sen and S. Dey, *Acta Crystallogr., Sect. C: Cryst. Struct. Commun.: Cryst. Struct. Commun.*, 2005, **61**, o358; (c) G. Mehta, S. Sen and K. Venkatesan, *CrystEngComm*, 2005, **7**, 398; (d) G. Mehta, S. Sen and S. S. Ramesh, *CrystEngComm*, 2005, **7**, 563; (e) G. Mehta and S. Sen, *CrystEngComm*, 2005, **7**, 656.
- (a) G. Mehta and S. S. Ramesh, *Chem. Commun.*, 2000, 2429; (b) G. Mehta and S. S. Ramesh, *Tetrahedron Lett.*, 2001, **42**, 1987.
- (a) G. A. Jeffrey and W. Saenger, *Hydrogen Bonding in Biological Structures*, Springer-Verlag, New York, 1991; (b) G. A. Jeffrey, *An Introduction to Hydrogen Bonding*, Oxford University Press, Oxford, UK, 1997.
- G. Mehta, S. Sen and S. S. Ramesh, *Eur. J. Org. Chem.*, 2006(ASAP).
- (a) J. Bernstein, R. J. Davey and J.-O. Henck, *Angew. Chem., Int. Ed.*, 1999, **38**, 3440; (b) J. Bernstein, *Polymorphism in Molecular Crystals*, Oxford University Press, Oxford, UK, 2002; (c) also see the special issue on polymorphism in *Cryst. Growth Des.*, 2004, **4**, 1085–1444.
- (a) S. Miyazaki, M. Nakano and T. Arita, *Chem. Pharm. Bull.*, 1976, **24**, 2094; (b) E. Staab, L. Addadi, L. Leiserowitz and M. Lahav, *Adv. Mater.*, 1990, **2**, 40; (c) I. Weissbuch, R. Popovitz-Biro, M. Lahav and L. Leiserowitz, *Acta Crystallogr., Sect. B: Struct. Sci.*, 1995, **51**, 115; (d) C. Sano, T. Kashiwagi, N. Nagashima and T. Kawakita, *J. Cryst. Growth*, 1997, **178**, 568; (e) M. Kitamura and T. Ishizu, *J. Cryst. Growth*, 1998, **192**, 225; (f) N. Blagden and R. Davey, *Chem. Br.*, 1999, **35**, 44; (g) X. He, J. G. Stowell, K. R. Morris, R. R. Pfeiffer, H. Li, G. P. Stahly and S. R. Byrn, *Cryst. Growth Des.*, 2001, **1**, 305; (h) C.-H. Gu, K. Chatterjee, V. Young and D. J. W. Grant, *J. Cryst. Growth*, 2002, **235**, 471; (i) R. J. Davey, K. Allen, N. Blagden, W. I. Cross, H. F. Lieberman, M. J. Quayle, S. Righini, L. Seton and G. J. T. Tiddy, *CrystEngComm*, 2002, **4**, 257; (j) R. Lakshminarayanan, S. Valiyaveetil and G. L. Loy, *Cryst. Growth Des.*, 2003, **3**, 953; (k) P. Agarwal and K. A. Berglund, *Cryst. Growth Des.*, 2004, **4**, 479; (l) P. K. Thallapally, R. K. R. Jetti, A. K. Katz, H. L. Carrell, K. Singh, K. Lahiri, S. Kotha, R. Boese and G. R. Desiraju, *Angew. Chem., Int. Ed.*, 2004, **43**, 1149 and references therein; (m) C. Cashell, D. Corcoran and B. K. Hodnett, *Cryst. Growth Des.*, 2005, **5**, 593; (n) P. Retailleau, N. Colloc'h, D. Vivarès, F. Bonneté, B. Castro, M. El Hajji and T. Prangé, *Acta Crystallogr., Sect. D: Biol. Crystallogr.*, 2005, **61**, 218; (o) J. M. Kelleher, S. E. Lawrence and H. A. Moynihan, *CrystEngComm*, 2006, **8**, 327; (p) O.-P. Kwon, S.-J. Kwon, M. Jazbinsek, A. Choubey, P. A. Losio, V. Gramlich and P. Günter, *Cryst. Growth Des.*, ASAP.
- (a) C. V. Krishnamohan Sharma and M. J. Zaworotko, *Chem. Commun.*, 1996, 2655; (b) R. J. Davey, N. Blagden, G. D. Potts and R. Docherty, *J. Am. Chem. Soc.*, 1997, **119**, 1767; (c) R. Liu, K.-F. Mok and S. Valiyaveetil, *New J. Chem.*, 2001, **25**, 890; (d) X.-L. Zhang and X.-M. Chen, *Cryst. Growth Des.*, 2005, **5**, 617; (e) M. Du, Z.-H. Zhang and X.-J. Zhao, *Cryst. Growth Des.*, 2005, **5**, 1247; (f) T. R. Shattock, P. Vishweshwar, Z. Wang and M. J. Zaworotko, *Cryst. Growth Des.*, 2005, **5**, 2046.
- DSC characteristics of the two polymorphs and DFT single point energy comparison in the packing motifs of the two forms of **2** have been included in the ESI.† Relevant details of molecular structure and packing in the  $\alpha$  form of **2** have also been appended.
- Crystal structures of the additives used in the present study have been reported in the following articles: (a) *Trimesic acid*: D. J. Duchamp and R. E. Marsh, *Acta Crystallogr., Sect. B: Struct. Crystallogr. Cryst. Chem.*, 1969, **25**, 5; (b) *Benzoic acid*: (i) G. Bruno and L. Randaccio, *Acta Crystallogr., Sect. B: Struct. Crystallogr. Cryst. Chem.*, 1980, **36**, 1711; (ii) R. Feld, M. S. Lehmann, K. W. Muir and J. C. Speakman, *Z. Kristallogr.*, 1981, **157**, 215; (iii) C. C. Wilson, N. Shankland and A. J. Florence, *J. Chem. Soc., Faraday Trans.*, 1996, **92**, 5051; (c) *Phthalic acid*: (i) H. Kuppers, *Cryst. Struct. Commun.*, 1981, **10**, 989; (ii) O. Ermer, *Helv. Chim. Acta*, 1981, **64**, 1902; (d) *Isophthalic acid*: (i) J. L. Derissen, *Acta Crystallogr., Sect. B: Struct. Crystallogr. Cryst. Chem.*, 1974, **30**, 2764; (ii) R. Alcalá and S. Martínez-Carrera, *Acta Crystallogr., Sect. B: Struct. Crystallogr. Cryst. Chem.*, 1972, **28**, 1671; (e) *Terphthalic acid*: (i) M. Bailey and C. J. Brown, *Acta Crystallogr.*, 1967, **22**, 387; (ii) A. Domenicano, G. Schultz, I. Hargittai, M. Colapietro, G. Portalone, P. George and C. W. Bock, *Struct. Chem.*, 1990, **1**, 107; (iii) M. Sledz, J. Janczak and R. Kubiak, *J. Mol. Struct.*, 2001, **595**, 77; (f) *Boric acid*: R. R. Shuvalov and P. C. Burns, *Acta Crystallogr., Sect. C: Cryst. Struct. Commun.*, 2003, **59**, i47; (g) *Phloroglucinol*: K. Maartmann-Moe, *Acta Crystallogr.*, 1965, **19**, 155; (h) *Cyanuric acid*: (i) G. C. Verschoor and E. Keulen, *Acta Crystallogr., Sect. B: Struct. Crystallogr. Cryst. Chem.*, 1971, **27**, 134; (ii) A. Kutoglu and E. Hellner, *Acta Crystallogr., Sect. B: Struct. Crystallogr. Cryst. Chem.*, 1978, **34**, 1617; (iii) H. Dietrich, C. Scheringer, H. Meyer, K.-W. Schulte and A. Schweig, *Acta Crystallogr., Sect. B: Struct. Crystallogr. Cryst. Chem.*, 1979, **35**, 1191; (iv) P. Coppens and A. Vos, *Acta Crystallogr., Sect. B: Struct. Crystallogr. Cryst. Chem.*, 1971, **27**, 146.
- In recent years, there has been an ongoing debate and discussion on the valid use of the qualifier "pseudopolymorph", see: (a) A. Nangia, *Cryst. Growth Des.*, 2006, **6**, 2; (b) J. Bernstein, *Cryst. Growth Des.*, 2005, **5**, 1661; (c) K. R. Seddon, *Cryst. Growth Des.*, 2004, **4**, 1087; (d) G. R. Desiraju, *Cryst. Growth Des.*, 2004, **4**, 1089.

- 
- 11 The Bravais–Friedel–Donnay–Harker (BFDH) law states the morphological importance of an  $\{hkl\}$  face is greater if the corresponding interplanar distance  $d_{hkl}$  is larger; see: (a) G. Wulff, *Z. Kristallogr.*, 1901, **34**, 449; (b) J. D. H. Donnay and D. Harker, *Am. Mineral.*, 1937, **22**, 446; (c) P. Hartman and W. G. Perdok, *Acta Crystallogr.*, 1955, **8**, 49.
- 12 (a) C. A. Mitchell, L. Yu and M. D. Ward, *J. Am. Chem. Soc.*, 2001, **123**, 10830; (b) M. Lang, A. L. Grzesiak and A. J. Matzger, *J. Am. Chem. Soc.*, 2002, **124**, 14834; (c) R. Hiremath, S. W. Varney and J. A. Swift, *Chem. Mater.*, 2004, **16**, 4948; (d) R. Hiremath, J. A. Basile, S. W. Varney and J. A. Swift, *J. Am. Chem. Soc.*, 2005, **127**, 18321.
- 13 W. C. McCrone, *Physics and chemistry of the organic solid state*, ed. D. Fox, M. M. Labes and A. Weissberger, Wiley Interscience, New York, USA, 1965, vol. 2, pp. 725–67.
- 14 M. J. Frisch, G. W. Trucks, H. B. Schlegel, G. E. Scuseria, M. A. Robb, J. R. Cheeseman, J. A. Montgomery, Jr., T. Vreven, K. N. Kudin, J. C. Burant, J. M. Millam, S. S. Iyengar, J. Tomasi, V. Barone, B. Mennucci, M. Cossi, G. Scalmani, N. Rega, G. A. Petersson, H. Nakatsuji, M. Hada, M. Ehara, K. Toyota, R. Fukuda, J. Hasegawa, M. Ishida, T. Nakajima, Y. Honda, O. Kitao, H. Nakai, M. Klene, X. Li, J. E. Knox, H. P. Hratchian, J. B. Cross, C. Adamo, J. Jaramillo, R. Gomperts, R. E. Stratmann, O. Yazyev, A. J. Austin, R. Cammi, C. Pomelli, J. W. Ochterski, P. Y. Ayala, K. Morokuma, G. A. Voth, P. Salvador, J. J. Dannenberg, V. G. Zakrzewski, S. Dapprich, A. D. Daniels, M. C. Strain, O. Farkas, D. K. Malick, A. D. Rabuck, K. Raghavachari, J. B. Foresman, J. V. Ortiz, Q. Cui, A. G. Baboul, S. Clifford, J. Cioslowski, B. B. Stefanov, G. Liu, A. Liashenko, P. Piskorz, I. Komaromi, R. L. Martin, D. J. Fox, T. Keith, M. A. Al-Laham, C. Y. Peng, A. Nanayakkara, M. Challacombe, P. M. W. Gill, B. Johnson, W. Chen, M. W. Wong, C. Gonzalez and J. A. Pople, *Gaussian 03, revision C.02*, Gaussian, Inc., Wallingford, CT, 2004.
- 15 *SMART (Version 6.028)*, *SAINTE (Version 6.02)*, *XPREP*, Bruker AXS Inc., Madison, WI, 1998.
- 16 G. M. Sheldrick, *SADABS*, University of Göttingen, Germany, 1996.
- 17 A. Altomare, G. Casciarano, C. Giacovazzo, A. Guagliardi, M. C. Burla, G. Polidori and M. Camalli, *J. Appl. Crystallogr.*, 1994, **27**, 435.
- 18 G. M. Sheldrick, *SHELXL97*, University of Göttingen, Germany, 1997.
- 19 L. J. Farrugia, *J. Appl. Crystallogr.*, 1997, **30**, 565.
- 20 D. M. Watkin, L. Pearce and C. K. Prout, *CAMERON - A Molecular Graphics Package*, Chemical Crystallography Laboratory, University of Oxford, 1993.
- 21 (a) I. J. Bruno, J. C. Cole, P. R. Edgington, M. K. Kessler, C. F. Macrae, P. McCabe, J. Pearson and R. Taylor, *Acta Crystallogr., Sect. B: Struct. Sci.*, 2002, **58**, 389–397; (b) C. F. Macrae, P. R. Edgington, P. McCabe, E. Pidcock, G. P. Shields, R. Taylor, M. Towler and J. van de Streek, *J. Appl. Crystallogr.*, 2006, **39**, 453.
- 22 M. Nardelli, *J. Appl. Crystallogr.*, 1995, **28**, 659.
- 23 A. L. Spek, *J. Appl. Crystallogr.*, 2003, **36**, 7.